Dendritic Integration and Its Role in Computing Image Velocity

Sandra Single and Alexander Borst*

The mechanisms underlying visual motion detection can be studied simultaneously in different cell compartments in vivo by using calcium as a reporter of the spatiotemporal activity distribution in single motion-sensitive cells of the fly. As predicted by the Reichardt model, local dendritic calcium signals are found to indicate the direction and velocity of pattern motion but are corrupted by spatial pattern properties. The latter are canceled out by spatial integration, thus leading to a purely directional selective output signal in the axon. These findings attribute a specific computational task to the dendrites of visual interneurons and imply a functional interpretation of dendritic morphology.

In the third optic neuropile of the blowfly *Calliphora erythrocephala* (lobula plate), there exist about 60 different, individually identifiable tangential cells (LPTCs) (*1*). Located directly underneath the rear surface of the brain, they are easily accessible after the head capsule has been opened and can be imaged in vivo (*2–4*) while being stimulated by motion (Fig. 1A). Among the LPTCs, cells are found that respond preferentially to vertical motion like the VS cells (*5*) as well as cells that are best activated by horizontal motion like the HS and CH cells (*6*). In general, LPTCs are involved in visual course control and show direction-selective motion responses by shifting their membrane potential as well as their intracellular calcium concentration (Fig. 1B). During preferred direction motion (PD), the cells depolarize in a graded way. This depolarization, sometimes superimposed by action potentials of small and irregular amplitude (*7*), is accompanied by an increase in the intracellular calcium concentration. During antipreferred or null direction motion (ND), the cells hyperpolarize and the calcium concentration decreases. As has been found in nine other LPTCs, the amplitude and time course of the electrophysiological and the calcium response always show a high degree of similarity (*8*). In addition to detecting the direction of motion, LPTCs also encode pattern velocity in the amplitude of their electrical response (*9*). To examine whether this also holds true for the intracellular calcium level, we measured the correlation between the overall dendritic calcium concentration and the membrane potential when stimulating LPTCs with pattern motion of different velocities. The results indicate a fairly linear relationship between axonal membrane potential and dendritic calcium concentration (*10*).

The LPTC response to visual motion can be formally described by the so-called Reichardt model of motion detection (*11, 12*). Reichardt detectors provide a direction-selective signal by correlating the luminance levels in adjacent retinal locations. They are assumed to be represented by small-field elements in the medulla, the second optic neuropile of the fly brain, impinging onto the dendrites of the LPTCs in a retinotopic way (*13, 14*). The output signals of the medulla elements, integrated by the LPTCs, lead to the characteristic response of the LPTCs representing the direction and velocity of pattern motion. According to the Reichardt model, a local input to the LPTCs should exhibit a two-component response: a constant shift and, superimposed on it, temporal modulations in phase with the local luminance of the pattern (*12*). By spatially integrating the output signals of many Reichardt detectors, the modulations are canceled, which results in a smooth graded response to constant image motion. To obtain a quantitative prediction of how strongly the dendritic membrane potential of the integrating neuron is expected to be locally modulated when fed with output signals of Reichardt-type motion detectors, we performed computer simulations on a compartmental model of a LPTC (Fig. 2). The anatomy of the cell was obtained from three-dimensional recon-

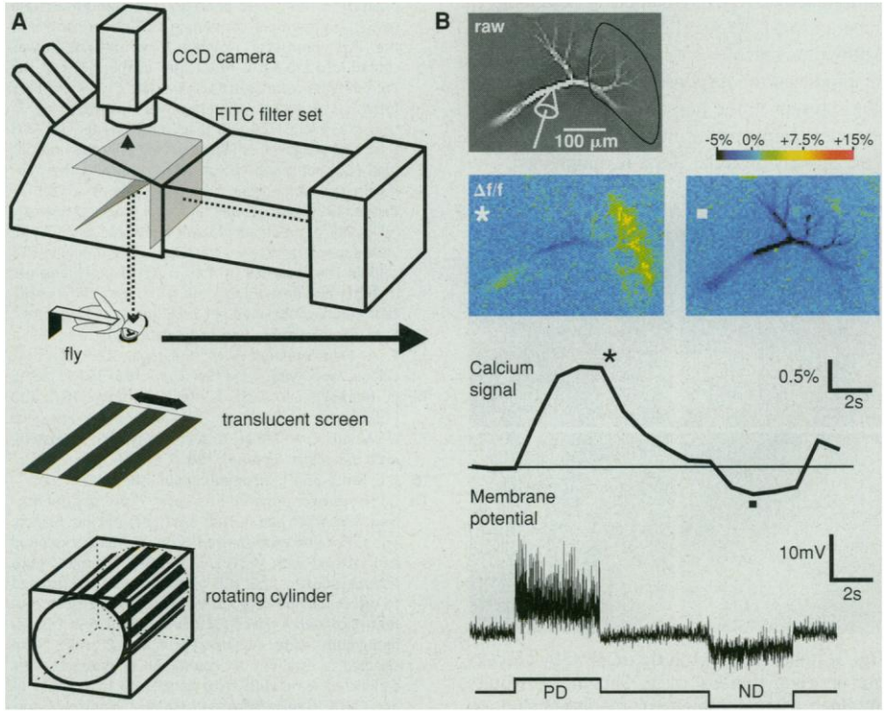

Fig. 1. (**A**) A fly is schematically shown viewing onto a moving grating beneath it. From above, after removal of one of the rear head capsules, LPTCs can be filled with calcium green and afterward be imaged by using an upright microscope and a CCD camera. (**B**) Calcium dynamics in a fly LPTC (VS1 cell) during visual stimulation in the cell's PD and ND with a velocity of 78° per second. Raw fluorescence and false-color images of the relative change of fluorescence ($\Delta f/f$) of the VS1 cell, during PD and ND motion, are shown above. The latter display the spatial distribution of the calcium signal in the VS1 cell during motion. The time course of the dendritic calcium signal of the cell along with the membrane potential recorded from its axon is presented below.

Friedrich-Miescher-Laboratory of the Max-Planck-Society, Spemannstrasse 37-39, D-72076 Tuebingen, Germany.

*To whom correspondence should be addressed. E-mail: alexander.borst@tuebingen.mpg.de

structions of cobalt-stained material, and the membrane parameters were derived from current and voltage clamp experiments (*15–17*). If such a neuron is synaptically driven by an array of Reichardt detectors stimulated by constant motion in the cell's preferred direction (downward), the dendritic membrane potential is locally modulated around a mean excitation level, whereas the axonal membrane potential consists of a constant shift only. The amplitude of the dendritic membrane potential modulations is about 20% of the mean excitation level, and the phase varies with the location in the dendrite. This is in accordance with the retinotopic arrangement of the input elements and their responses to the local luminance changes of the pattern. The exact time course is discussed below.

The demonstration of a linear relationship between membrane voltage and intracellular calcium concentration suggests that the intracellular calcium concentration of LPTCs is controlled by membrane voltage. For that reason we used calcium green as a reporter of dendritic activity to compare the behavior of the simulated cell with the behavior of a real cell (Fig. 3). Evaluating the time course of local calcium changes in small dendritic areas during constant PD motion, we found that the calcium signal in these areas was permanently increased and, in addition, modulated with the temporal frequency of the stimulus. In different areas of the dendrite, these modulations had a different phase offset. Similar results were obtained in 10 other experiments. The calcium modulations indicate local modulations of dendritic activity that are in phase with the retinal luminance level at the corresponding locations. In contrast to the activity modulations in the dendrite, the calcium signal in the axon showed a smooth time course, corresponding to the smooth axonal membrane potential. These data confirm the predictions derived from the Reichardt scheme of motion detection and closely match the results of the compartmental model simulations (Fig. 2).

The local dendritic calcium modulations unambiguously demonstrate local activity modulations in the dendrite. However, whether they reflect synaptic input activity only or local changes of postsynaptic membrane potential as well remains a question. Although the existence of voltage-activated calcium channels (VACCs) in the dendrites of LPTCs has been demonstrated (*4*), an additional calcium flux through transmitter-gated channels during synaptic stimulation cannot be excluded. This possibility must be considered in particular because nicotinic acetylcholine receptors (nAChRs) have been demonstrated on LPTCs (*14*), which, in vertebrates, are known to be permeable for calcium (*18*). Yet, for insect nAChRs, calcium permeability has not been tested (*19*). To decide whether the local calcium modulations in the dendritic tips are caused by VACCs and therefore directly represent local membrane modulations or whether the calcium signals repre-

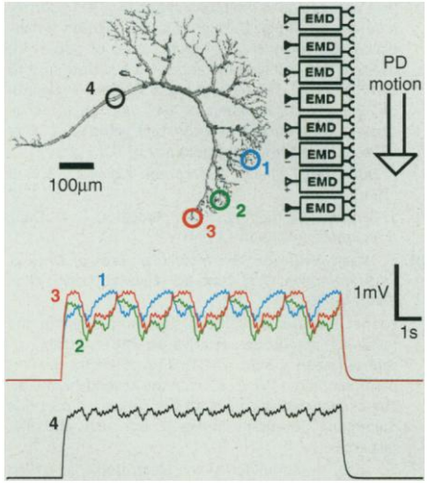

Fig. 2. (Top) A VS1 cell that was three-dimensionally reconstructed and used as a compartmental model to predict the spatio-temporal membrane potential distribution upon constant visual motion in the cell's PD (downward). The neuron is simulated to receive synaptic input from an array of Reichardt-type or EMDs. (Bottom) Resulting local membrane potentials in three dendritic areas indicated by the corresponding colors are shown together with the axonal membrane potential. Although the local dendritic potentials consist of a constant response superimposed by temporal modulations of identical frequency but various phase offsets, the axon potential is rather smooth.

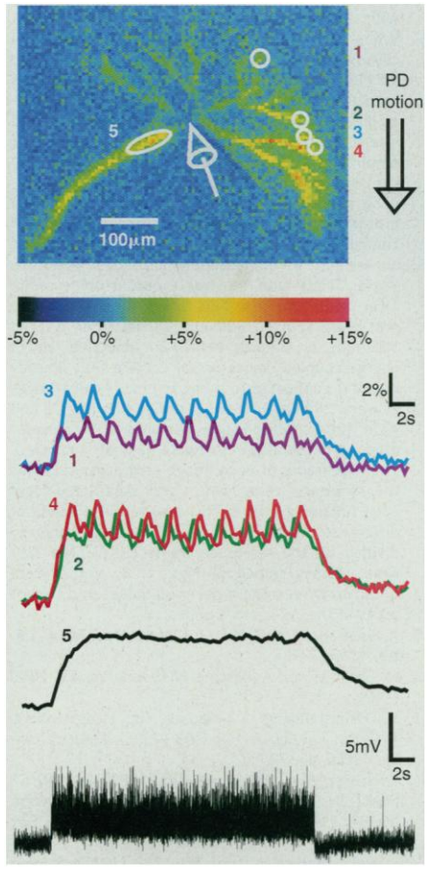

Fig. 3. Dendritic calcium modulations in a VS1 cell observed during constant image motion of a periodic grating in the cell's PD (downward). Image velocity was 13° per second, resulting in a temporal frequency of 0.5 Hz. (Top) One $\Delta f/f$ image of the cell is shown indicating the overall calcium response and the five areas in which the time course of relative fluorescence changes were evaluated. These time courses are displayed on the bottom in the corresponding colors together with the membrane potential. The fluorescence traces are modulated with the temporal frequency of the moving pattern and are phase shifted according to the location of the respective areas in the dendritic tree.

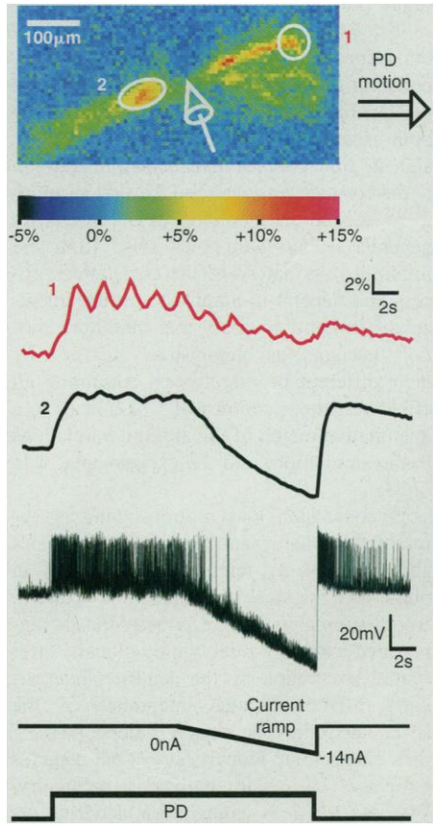

Fig. 4. Dendritic calcium modulations in an HS cell observed during constant image motion of a periodic grating in the cell's PD (from the front to the back of the animal). All the stimulus parameters were identical to the experiment shown in Fig. 3. In addition, a negative current ramp (0 to −14 nA) was applied in the second half of the stimulation interval. This led to a decreased amplitude of the calcium modulations.

sent modulated synaptic input activity only, we applied the same stimulus protocol as in Fig. 3 with one modification: after 10 s of PD motion, a negative current ramp was applied simultaneously to the continuing PD motion stimulus. If nAChRs are the only gate for calcium to enter the cell, then the amplitude of the modulation should increase by hyperpolarization of the cell. If, however, calcium is entering the cell via VACCs, the amplitude of the modulation should become reduced during hyperpolarization. The result from such an experiment performed on an HS cell is shown in Fig. 4. During the first 10 s of PD motion, the cell shows the typical dendritic calcium modulations. After the onset of the negative current ramp, the modulations become smaller with increasing amplitude of the hyperpolarizing current. We conclude that dendritic calcium modulations in LPTCs during PD motion are largely mediated by VACCs. Therefore, local calcium modulations observed during constant image motion (Fig. 3) are likely to reflect local dendritic membrane potential modulations.

Knowing the origin of the dendritic calcium response allows for a quantitative comparison of the simulation results (Fig. 2) and the local calcium measurements (Fig. 3). In both cases, close inspection of the dendritic signals' time courses reveals that, in addition to the constant response and the first harmonic, a second harmonic is also present. In general, second harmonics arise from the multiplicative nature of the correlation process and depend in amplitude on the imbalance between excitatory and inhibitory motion detectors, as biophysically realized by their different driving forces. Assuming an effective pattern contrast of 3 (*12*) leads to a quantitative match of the amplitude relations in the simulations and the experimental data (*20*).

In conclusion, local motion signals as represented by the synaptic inputs to fly LPTCs are corrupted by temporal modulations in phase with the local luminance of the pattern. Information about image velocity thus is represented with high fidelity only globally after spatial integration by the dendrite. Interestingly, effective spatial integration by the LPTC dendrites is almost independent of their electrotonic properties (*21*) but depends critically on their particular geometry. Whereas VS cells extend their dendritic arbors mainly along the dorsoventral axis of the lobula plate, dendrites of horizontal-sensitive HS and CH cells are much more oriented along the medial-lateral axis. Because the orientation of the dendritic arbor is aligned with that direction of motion where temporal modulations are phase offset, the modulations are optimally canceled by spatial integration. The respective geometries of the LPTC dendrites thus appear to support the specific computational task of the neurons in visual course control.

References and Notes

1. K. Hausen, *Photoreception and Vision in Invertebrates*, M. A. Ali, Ed. (Plenum, New York, 1984), p. 523.
2. Preparation and setup: Female blowflies (*C. erythrocephala*) were prepared as described in (*17*). Visual stimuli were produced by a grating drum illuminated from the inside by an arc lamp, the image of which was projected onto a screen (10 × 8 cm) positioned 10 cm below the fly (Fig. 1A). The fly was mounted to look down on the stimulus and the objective was above the back of its opened head capsule. The square wave grating had a spatial wavelength of 26°, a mean luminance of 17.7 cd/m^2, and a contrast of 92%. The velocity of the moving pattern depended on the type of experiment and is indicated in the figure legends. Electrophysiological recording: Electrodes were pulled on a Brown-Flaming micropipette puller (P-97, Sutter Instruments) using thin-wall glass capillaries with a diameter of 1 mm (GC100TF-10, Clark). When filled with 2 M KAc, 0.5 M KCl, and 8.8 mM calcium green, they had resistances of about 30 to 40 MΩ. A SEC-10L amplifier (npi-electronics) was used throughout the experiments and was operated in the Bridge or discontinuous current clamp mode. For data analysis, the output signal of the amplifier was fed to a PC 486 via a 12-bit A/D converter (CIO-DAS16, ComputerBoards) at a sampling rate of 3 kHz and stored to hard disc. The motor control unit for the rotating cylinder was controlled by a PC 468. Optical recording: We used an upright epifluorescent microscope (Axiotech Vario, Zeiss) with the fluorescein isothiocyanate filter set 9 from Zeiss (excitation filter, 450 to 490 nm; beam splitter, 510 nm; barrier filter, 516 to 565 nm), an Epiplan ×10/0.20 objective, and a charge-coupled device (CCD) camera (PXL, Photometrics) connected to a Power-Mac (Apple). Images were taken at 1 Hz (Fig. 1) or at 4 Hz (Figs. 3 and 4) at 128 × 128 pixel resolution and were evaluated with the IPLab software (Signal Analytics). The first frame of each image series was taken as the reference frame, which was subtracted from each following image. This resulted in a series of difference images (Δf), which were subsequently divided by the reference frame ($\Delta f/f$). The $\Delta f/f$ time courses shown in Figs. 1, 3, and 4 were obtained by averaging the pixel values in different areas in the $\Delta f/f$ image series.
3. A. Borst and M. Egelhaaf, *Proc. Natl. Acad. Sci. U.S.A.* **89,** 4139 (1992).
4. M. Egelhaaf and A. Borst, *J. Neurophysiol.* **73,** 2540 (1995).
5. R. Hengstenberg, K. Hausen, B. Hengstenberg, *J. Comp. Physiol. A* **149,** 163 (1982); R. Hengstenberg, *ibid.*, p. 179.
6. K. Hausen, *Biol. Cybern.* **45,** 143 (1982); *ibid.* **46**, 67 (1982); H. Eckert and D. R. Dvorak, *J. Insect Physiol.* **29,** 547 (1983); K. Hausen, *Z. Naturforsch.* **31c,** 629 (1976).
7. R. Hengstenberg, *Nature* **270,** 338 (1977); J. Haag and A. Borst, *ibid.* **379,** 639 (1996).
8. The decrease in calcium concentration during hyperpolarization is indicative of a partial activation of VACCs at the cell's resting potential. This has in fact been directly measured for the CH cells in voltage clamp experiments (*15*). The calcium current showed little inactivation and its activation characteristic was rather flat, with about 30% of maximum current at resting potential.
9. J. Haag and A. Borst, *J. Neurosci.* **17,** 4809 (1997).
10. Four different LPTCs were visually stimulated by gratings moving at a constant velocity of 15.6°, 52°, 156°, and 234° per second. Although each of the cells showed differences in response strength, the relationship between membrane potential and dendritic calcium concentration was fairly linear with an average correlation coefficient of 0.92 ± 0.05 (mean ± SEM).
11. W. Reichardt, in *Sensory Communication*, W. A. Rosenblith, Ed. (M.I.T. Press and Wiley, New York, 1961), p. 303; W. H. Zaagman, H. A. K. Mastebroek, J. W. Kuiper, *Biol. Cybern.* **31,** 163 (1978); W. Reichardt, *J. Comp. Physiol. A* **161,** 533 (1987); M. Egelhaaf and A. Borst, *Vis. Neurosci.* **8,** 151 (1992); D. O'Carroll, N. J. Bidwell, S. B. Laughlin, E. J. Warrant, *Nature* **382,** 63 (1996).
12. M. Egelhaaf, A. Borst, W. Reichardt, *J. Opt. Soc. Am. A* **6,** 1070 (1989).
13. E. Buchner, S. Buchner, I. Bülthoff, *J. Comp. Physiol. A* **155,** 471 (1984); J. K. Douglass and N. J. Strausfeld, *J. Neurosci.* **15,** 5596 (1995); S. Single, J. Haag, A. Borst, *ibid.* **17,** 6023 (1997).
14. T. M. Brotz and A. Borst, *J. Neurophysiol.* **76,** 1786 (1996).
15. J. Haag, F. Theunissen, A. Borst, *J. Computat. Neurosci.* **4,** 349 (1997).
16. Compartmental modeling: Cells were reconstructed as described in (*17*). For the neuron shown in Fig. 2, a so-called VS1 cell, the anatomical data file consisted of about 1600 entry points. Assuming spatially uniform parameters, the passive membrane properties amounted to 2.0 kΩcm^2 for the specific membrane resistance R_m, 40 Ωcm for the internal resistivity R_i, and 0.8 μF/cm^2 for the membrane capacity C_m. The Nemosys simulation software package (*22*) was used to calculate the time course of the membrane potential for each compartment of the neuron. In the simulation shown here, the neuron was driven synaptically by an array of 32 excitatory and 32 inhibitory correlation type or elementary motion detectors (EMDs). Each such detector consisted of two inputs measuring the local light intensity in two neighboring locations of the pattern spaced by 2° of visual angle, one first-order low-pass filter with τ = 100 ms, and a nonlinear interaction stage where the filtered signal from one location was multiplied by the instantaneous signal from the neighboring location. One array of such detectors provided excitatory input to the neuron (E_{rev} = +40 mV relative to resting) and the other array, a mirror image of the first one, provided inhibitory input (E_{rev} = −30 mV relative to resting). During visual stimulation synaptic conductances reached peak levels of about 1.0 nS/cm^2. The postsynaptic areas had a surface of 3 to 9 × 10^{-6} cm^2. The pattern had a spatial wavelength of 32°, a vertical extent of 64°, and an effective contrast of 3, moving at a constant velocity of 16°/s to result in a temporal frequency of 0.5 Hz.
17. A. Borst and J. Haag, *J. Computat. Neurosci.* **3,** 313 (1996).
18. S. Vernino, M. Rogers, K. A. Radcliffe, J. A. Dani, *J. Neurosci.* **14,** 5514 (1994).
19. H. Breer, *Neurotox '88: Molecular Basis of Drug & Pesticide Action*, G. G. Lunt, Ed. (Elsevier, Amsterdam, 1988), p. 301.
20. Fourier analysis of calcium signals resulted in the following amplitudes relative to the constant response (mean ± SEM; n = 4): 21% ± 4% for the first harmonic and 11% ± 2% for the second harmonic. The corresponding values for the simulated dendritic membrane potentials in Fig. 2 are 18% and 8%, respectively.
21. To study the influence of the electrotonic length on the spatial integration properties, we varied the ratio of membrane resistance and internal resistivity, R_m/R_i, by factors of 0.25 and 4 compared to the values used for the simulation in Fig. 2. These variations had a strong influence on the amplitudes of the local membrane modulations, with the latter being almost absent in case of large R_m/R_i ratios. However, there was no effect on the cancellation of the local input modulations by dendritic integration, resulting in a smooth axonal signal in each case.
22. F. H. Eeckman, F. E. Theunissen, J. P. Miller, in *Neural Network Simulation Environments*, J. Skrzypek, Ed. (Kluwer Academic, Boston, 1994), p. 114.

23. We are grateful to H. Nguyen for excellent technical assistance and to T. Brotz, J. Haag, and T. Oertner for critically reading the manuscript.

8 June 1998; accepted 17 August 1998